Structure, Redox Chemistry, and Interfacial Alloy Formation in Monolayer and Multilayer Cu/Au(111) Model Catalysts for CO2 Electroreduction

ARTICLE *in* THE JOURNAL OF PHYSICAL CHEMISTRY C · APRIL 2014

Impact Factor: 4.77 · DOI: 10.1021/jp412000j

10 AUTHORS, INCLUDING:

Daniel Friebel
Stanford University
32 PUBLICATIONS **461** CITATIONS
SEE PROFILE

Hirohito Ogasawara
Stanford University
142 PUBLICATIONS **5,192** CITATIONS
SEE PROFILE

Roberto Alonso-Mori
Stanford University
66 PUBLICATIONS **960** CITATIONS
SEE PROFILE

Dennis Nordlund
Stanford University
188 PUBLICATIONS **4,627** CITATIONS
SEE PROFILE

THE JOURNAL OF PHYSICAL CHEMISTRY C

Article

pubs.acs.org/JPCC

Structure, Redox Chemistry, and Interfacial Alloy Formation in Monolayer and Multilayer Cu/Au(111) Model Catalysts for CO_2 Electroreduction

Daniel Friebel,*[,†] Felix Mbuga,[†] Srivats Rajasekaran,[†] Daniel J. Miller,[†] Hirohito Ogasawara,[‡] Roberto Alonso-Mori,[‡] Dimosthenis Sokaras,[‡] Dennis Nordlund,[‡] Tsu-Chien Weng,[‡] and Anders Nilsson[†,‡]

[†]SUNCAT Center for Interface Science and Catalysis, SLAC National Accelerator Laboratory, 2575 Sand Hill Rd., Menlo Park, California 94025, United States

[‡]Stanford Synchrotron Radiation Light Source (SSRL), SLAC National Accelerator Laboratory, 2575 Sand Hill Rd., Menlo Park, California 94025, United States

ABSTRACT: High-energy-resolution fluorescence-detection X-ray absorption spectroscopy (HERFD XAS) has been used to probe the geometric and electronic structure of a Cu monolayer model electrocatalyst as a function of applied potential *in situ* in alkaline electrolyte. In 0.01 M NaOH, a Cu monolayer deposited on an Au(111) single crystal exhibits markedly different redox behavior from Cu multilayers on the same substrate: the Cu monolayer is more stable against oxide formation and, at high potentials (E > 0.5 V vs RHE), undergoes a direct phase transition from Cu^0 to CuO rather than forming an intermediate Cu_2O phase. The Cu monolayer in its metallic state at low potentials is expanded by 12.5% to match the substrate lattice constant, which can be expected to influence significantly the interaction of Cu surface atoms with intermediates of the electrochemical CO_2 reduction. However, we also find that both strained Cu monolayer and thick, structurally relaxed Cu islands are unstable with respect to place-exchange with subsurface Au atoms. Such segregation phenomena need to be carefully considered and can limit the applicability of lattice strain as independent catalyst design parameter.

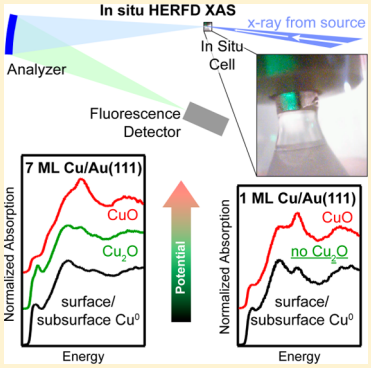

INTRODUCTION

The discovery of a new electrocatalyst that efficiently converts CO_2 into liquid fuels and feedstock chemicals could allow our hydrocarbon-based energy and materials infrastructure to become sustainable. To date, however, metal electrodes that have been shown to reduce CO_2 require very large (~1 V) overpotentials and lack selectivity for CO_2 reduction over H_2 evolution.[1,2] Copper is the most promising candidate among pure metals, in particular due to its unique ability to catalyze the formation of hydrocarbons. Although various attempts have been made to improve activity and selectivity, e.g. by pretreatment of Cu electrodes involving Cu oxide formation[3,4] or by introducing strain,[5] its performance remains unsatisfactory with respect to both overpotential and product distribution.[1,2] Recently, Cu/Au alloys were reported to have improved faradaic efficiencies for CO_2 reduction compared to both parent metals; at the same time, however, even small (10%) additions of Au were found to completely suppress hydrocarbon formation, giving rise instead to highly selective formation of CO.[6]

The rational design of a Cu catalyst with optimized activity and selectivity requires that one first study structurally well-defined model catalysts[5,7] that allow changes in reactivity to be correlated with a small set of material parameters, e.g., lattice strain, crystallographic orientation, and d-band occupancy. In addition to these global parameters that are assumed to influence adsorption energies homogeneously over the entire catalyst surface, the tailored design of local variances from an average structure, such as nanostructured islands with locally enhanced catalytic activity,[8] replacement of individual surface atoms, or generation of well-defined atomic ensembles with unique functionality,[9−12] is a promising approach toward new electrocatalysts with significantly enhanced activity and selectivity. An especially useful model system for studying effects of lattice strain and bimetallic interactions is a single atomic layer of Cu deposited on a low-index, single-crystal surface of a foreign host metal.[7] The most attractive feature of such a system for catalytic studies is that all surface atoms have the same local coordination environment and therefore identical site-specific catalytic activity. Furthermore, element-sensitive X-ray absorption spectroscopy at high X-ray energies (>8 keV) can probe such a catalyst *in situ* even under millimeter-thick electrolyte,[8,13−17] and this inherently bulk sensitive technique will probe surface atoms exclusively when the absorbing element is deposited as a single atomic layer.[8,15] Our present study aims at exploring the electronic structure of

Received: December 7, 2013
Revised: March 14, 2014
Published: March 20, 2014

such a Cu monolayer on an Au(111) substrate under alkaline electrochemical conditions (0.01 M NaOH), using *in situ* high-energy-resolution fluorescence-detection X-ray absorption spectroscopy (HERFD XAS). We show that the redox behavior of Cu drastically changes due to Cu−Au interactions. Cu monolayers on Au(111) are significantly more stable against oxide formation at high potentials than are bulk Cu electrodes: with respect to a Cu/Au(111) multilayer, the onset of oxidation is anodically shifted on the monolayer Cu sample. Moreover, whereas the Cu multilayer clearly exhibits two successive Cu/Cu_2O and Cu_2O/CuO redox transitions, the monolayer deposit is directly oxidized from Cu^0 to CuO.

Furthermore, we present evidence for an instability of a Cu surface layer on Au(111) with respect to subsurface alloy formation. This process has received relatively little attention while its reversal, electrochemical dealloying of Cu−Au alloys during selective Cu dissolution,[18−22] and also adsorbate-driven segregation of Cu to the surface,[23,24] has been extensively studied. HERFD XAS shows that an increasing fraction of the Cu monolayer becomes inert against oxide formation. Likewise, the 7 ML thick Cu layer changes its structure in the metallic state, with an expansion of its lattice constant that indicates a transition from pure Cu toward a Cu/Au alloy. Accordingly, we propose here that phase-segregation phenomena must be carefully considered when designing Cu−Au alloys for CO_2 electroreduction.

EXPERIMENTAL METHODS

A commercial Au(111) single-crystal (hat-shaped with 4 mm diameter on the polished side, MaTecK, Jülich, Germany) was electrochemically oxidized at +10 V with respect to a Pt counter electrode in order to remove trace metal contaminations, followed by flame annealing with a butane torch. The crystal was then mounted inside a hanging-meniscus electrochemical cell for *in situ* grazing-incidence XAS,[8,14−17] which consists of a poly(ether ether ketone) (PEEK) tube with the electrolyte and ports for electrolyte delivery as well as counter and reference electrodes. A long highly coiled Pt wire was used as the counter electrode, and another Pt wire was used as pseudoreference electrode. All potentials are converted and stated with respect to the reversible hydrogen electrode (RHE). Contact with the working electrode is established through a free-standing meniscus in the 2 mm narrow gap between the tube and the sample surface.

Ultrathin Cu layers on Au(111) were prepared by carefully electrodepositing the desired amount of Cu from a 5 mM $CuSO_4$/50 mM H_2SO_4 solution, which was immediately followed by two electrolyte exchanges in order to first purge all remaining Cu^{2+} ions from the solution phase and then replace the acidic H_2SO_4 electrolyte with alkaline 0.01 M NaOH solution. This was accomplished by first exposing the crystal to the Cu deposition electrolyte at +0.65 V, well above the potentials for Cu under- and overpotential deposition. A cathodic linear sweep of the potential was then initiated while the deposition current was monitored. After completely passing the current features that correspond to the desired Cu upd coverage (first upd peak: 0.67 ML; second upd peak: 1.0 ML), the electrochemical cell was rapidly flushed with blank 0.05 M H_2SO_4 solution. Meanwhile, in order to prevent Cu dissolution as a result of Cu^{2+} depletion in the electrolyte, the cathodic potential sweep was continued until the potential was at least 0.15 V lower than at the beginning of the electrolyte exchange. The potential was then held constant with respect to the Pt pseudoreference electrode while the second electrolyte exchange was carried out.

Electrolytes were made from solid NaOH·H_2O (Suprapur, EMD Chemicals Inc.), 95% H_2SO_4 (Trace Select, Sigma-Aldrich), 99.999% $CuSO_4$·$5H_2O$ (Sigma-Aldrich), and ultrapure water from a Millipore Gradient system.

The Cu multilayer sample was made in similar fashion, except that flushing of the cell was started much later during the cathodic potential sweep when the bulk Cu deposition current approached the diffusion limit. The resulting thickness of the Cu deposit of 7.0 ± 0.2 ML was determined from the transferred charge, using the area of both upd peaks as internal calibration for 1 ML Cu. This value is in perfect agreement with an independent thickness determination using the X-ray fluorescence intensities from the two different samples.

All X-ray measurements were carried out at Beamline 6-2 of the Stanford Synchrotron Radiation Lightsource (SSRL) which has HERFD XAS capabilities.[25] A Si(311) monochromator in combination with an array of five spherically bent Si perfect crystals (R = 1 m) was used. The crystals were aligned in a Johann-type backscattering geometry[26] using the (444) Bragg reflection at 79.32° to select the Cu $K\alpha_1$ fluorescence line (8047.8 eV). The incidence angle of the X-ray beam to the Cu/Au(111) surface was adjusted to the critical angle (0.5°) for total external reflection, thereby enhancing the fluorescence intensity up to 4-fold.[27] The orientation of the electric field vector of the incident beam was perpendicular to the surface normal.

Since the attenuation length of the incident beam at energies near the Cu K absorption edge is only ∼1.4 mm in water, using a sample with larger diameter than in this study (4 mm) would not significantly improve the fluorescence yield.

RESULTS AND DISCUSSION

Strain Relaxation in Multilayer Cu Islands on Au(111). The structure of Cu upd layers on low-index surfaces of noble metals is generally assumed to be pseudomorphic; i.e., a single Cu monolayer adapts its lattice constant in registry with the substrate. In the present Cu/Au case the lattice mismatch is ∼12.5%, and this should result in a significantly strained Cu adlayer that is most unlikely. The unusual stability of an interface with such significant strain could be explained based on interactions of electrolyte anions with the Cu layer.[28] Additional structures have been reported, in which Cu atoms are even more widely spaced, such as the $(\sqrt{3} \times \sqrt{3})R30°$ honeycomb structure containing two Cu atoms and one coadsorbed sulfate anion per unit mesh,[29−31] and incommensurate layers sometimes referred to as "two-dimensional compound" layers of Cu halides[32] or sulfides.[33−35]

Figure 1 shows a comparison of HERFD XAS measurements for 1 and 7 ML Cu on Au(111) at potentials significantly below the stability range for bulk Cu oxides. By comparison with the conventional XAS (recorded in transmission mode) of Cu foil, it can be clearly seen that Cu is in the metallic state. The effect of partial removal of the lifetime broadening in HERFD results in spectral sharpening,[36−38] which becomes the most apparent in feature A^0. It is also noteworthy that the HERFD technique completely removes the elastic and Compton background. This is an enormous advantage for electrochemical studies where scattered intensity from the liquid electrolyte is typically one order of magnitude higher than the desired fluorescence signal.

The most striking difference between the spectra in Figure 1 is that features B^0, C^0, and D^0 are shifted to much lower

dx.doi.org/10.1021/jp412000j | J. Phys. Chem. C 2014, 118, 7954−7961

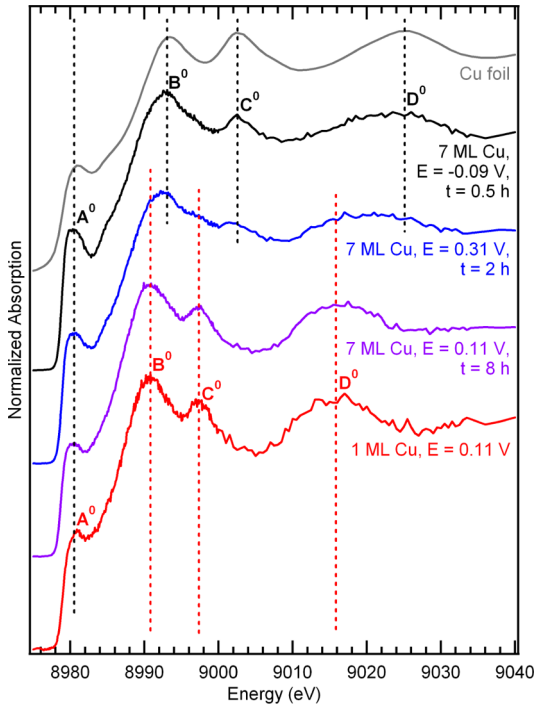

Figure 1. *In situ* HERFD XAS of Cu layers on Au(111) with two different thicknesses, 1 and 7 ML, in 0.01 M NaOH. For comparison, the transmission mode XANES of Cu foil is also shown. The structure-sensitive peaks B^0, C^0, and D^0 can be interpreted with an fcc structure of the Cu overlayer. The vertical dashed lines mark peak positions that correspond to the lattice spacing of bulk Cu (black dashed lines) or to a substrate-induced lattice expansion (red dashed lines) of the Cu layer. The spectrum for 7 ML Cu/Au(111) initially resembles the structure of the Cu foil, shows contributions from both bulk Cu and expanded structures after 2 h, and eventually becomes dominated by the features of the expanded lattice.

energies for 1 ML Cu/Au(111) than for the Cu foil reference. Using the "bond length with a ruler" concept,[39−41] these energy shifts can be qualitatively interpreted with an expansion of Cu−Cu bond lengths, indicating that the Cu monolayer retains its pseudomorphic (1 × 1) structure also in in 0.01 M NaOH. In fact, if we rescale the measured energies E_{exp} of the 1 ML Cu/Au(111) spectrum using the equation

$$E_S - E_0 = (E_{exp} - E_0)\frac{{d_{Au}}^2}{{d_{Cu}}^2} \quad (1)$$

with the Cu 1s photoionization threshold E_0 = 8978.9 eV[42] and the bulk nearest-neighbor distances of Cu and Au metals (d_{Cu} = 2.56 Å, d_{Au} = 2.88 Å), we obtain a curve that resembles closely the XANES of Cu foil (Figure 2). The onset of absorption is also identical within the accuracy of measurement for 1 ML Cu/Au(111) and bulk Cu, indicating only a very small chemical shift of the 1s core level. Therefore, we conclude that the Cu monolayer is in the metallic state and that its spectral changes compared to bulk Cu are mostly due to the geometric rather than electronic structure. It is important to note that, based on the observation of an expanded lattice constant for 1 ML Cu/Au(111) alone, we cannot rule out the possibility that some of the Cu atoms may have migrated to subsurface sites of the Au substrate. The short energy range of the HERFD XAS measurement is not sufficient for a detailed analysis of the energy dispersion of the photoelectron backscattering, which

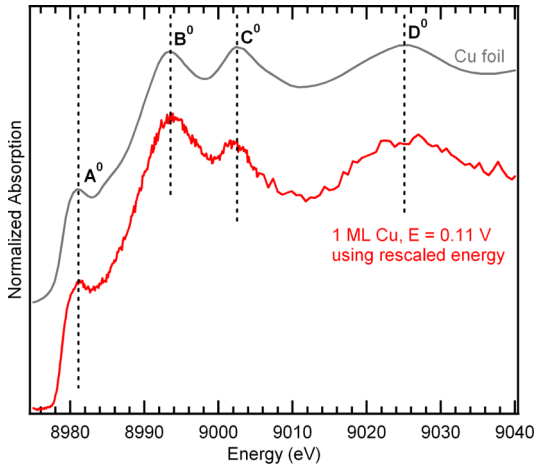

Figure 2. Comparison of bulk Cu XANES and *in situ* HERFD XAS of 1 ML Cu/Au(111), the latter being plotted against rescaled energy values using eq 1.

could be used to distinguish contributions from Cu and Au nearest neighbors. Circumstantial evidence that interfacial Cu/Au alloy formation indeed occurs can be obtained from our study of the reactivity of 1 ML Cu/Au(111) toward Cu oxide formation, which will be discussed in detail later.

Significant structural differences are apparent between 1 ML Cu/Au(111) and 7 ML Cu/Au(111) at low potentials. In the latter case, the spectra *initially* are almost identical with that of bulk Cu. Hence, most of the Cu atoms are fully relaxed toward the bulk Cu lattice parameters already at this rather low film thickness. Cu electrodeposition on Au(111) can be characterized as Stranski−Krastanov growth mechanism where multilayer islands grow on top of the upd monolayer.[43] Therefore, already at small multilayer coverages such as the 6.8 ML given here, only a small fraction of Cu atoms will be directly influenced by nearest-neighbor interactions with the Au substrate.

We note, however, that the spectral appearance of the multilayer Cu/Au(111) sample slowly changes over the course of the experiment. After ca. 2 h, additional spectral features appear at positions identical to those for 1 ML Cu coverage. These features, indicative of Cu in an expanded lattice, completely dominate the spectra after 8 h. Since there is no loss in spectral intensity that would indicate Cu dissolution, we propose that the growing Cu fraction with increased lattice spacing mostly consists of Cu atoms that have diffused into the Au substrate to form a near-surface alloy. The driving force for the underlying Cu−Au place-exchange is the significant lattice mismatch between the Au substrate along with the first, pseudomorphic Cu layer and the overlying thick Cu islands.

Here it is not yet known if there is the possibility of an additional effect of a particular electrochemical treatment (e.g., potential cycling or prolonged exposure under oxidizing or reducing conditions), which could result in an acceleration, inhibition, or even reversal of Cu−Au place-exchange.

Since alloy formation eventually, as seen in HERFD XAS after 8 h, appears to consume the entire 7 ML Cu deposit, and Au is well-known to have lower surface energy than Cu,[44] it is reasonable to assume that the electrode surface will be terminated mostly with Au surface atoms. This could explain why even a small addition (10%) of Au to a Cu electrocatalyst for CO_2 reduction results already in the complete inhibition of

dx.doi.org/10.1021/jp412000j | J. Phys. Chem. C 2014, 118, 7954−7961

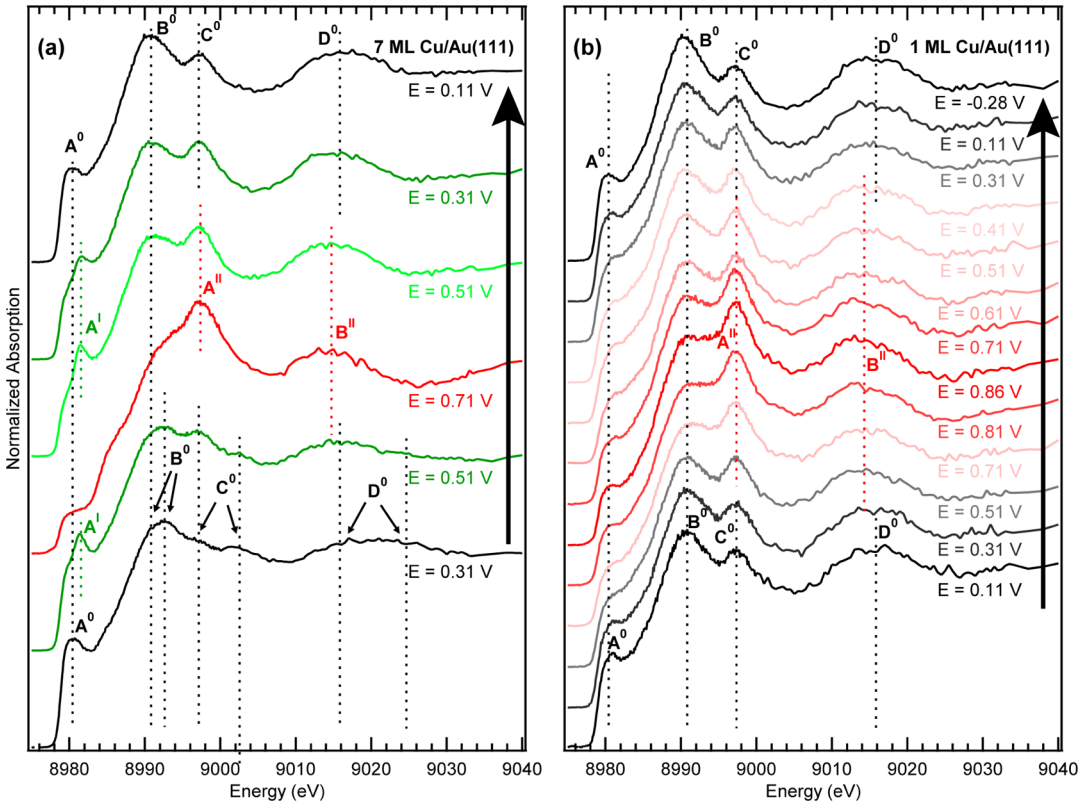

Figure 3. HERFD XAS of Cu/Au(111) recorded at a series of potentials, following the anodic oxidation of Cu and, subsequently, its reduction back to Cu^0. The Cu coverages are (a) 7 ML and (b) 1 ML. Each spectrum was measured after potential cycles between (a) 0.0 and 1.15 V and (b) −0.2 and 1.1 V, with the potential being held at the value indicated. Characteristic spectral features are labeled $A^0/B^0/C^0/D^0$ for Cu^0, A^I for Cu_2O, and A^{II}/B^{II} for CuO.

hydrocarbon formation and instead highly selective production of CO, quite similar to the characteristics of a pure Au catalyst.[6]

Influence of Cu Coverage on Redox Phase Transitions of Cu/Au(111). Electrochemical oxide growth on thick Cu electrodes has been well characterized using chemically sensitive *ex situ* XPS,[45−47] structure-sensitive *in situ* STM,[48−50] and surface X-ray diffraction.[51] Using *in situ* STM, ordered hexagonal superstructures were observed on Cu(111) in a narrow potential range below the onset of Cu oxide growth.[48] Comparison of the amount of charge transfer and estimated coverage as well as surface-enhanced Raman spectra both indicate that the adsorbed species is OH, not O.[48,52] DFT calculations predict that chemisorbed O on Cu(111), even at very low coverages, would be less stable than a O−Cu−O trilayer "surface oxide", which quite strongly resembles the bulk structure of Cu_2O.[53,54]

In good agreement with the Pourbaix diagram for Cu,[55] it has been consistently found that Cu oxidation in alkaline electrolytes commences with the growth of a cuprous oxide layer, followed by formation of an outer layer of mixed cupric oxides and hydroxides.[45−47] HERFD XAS of 7 ML Cu/Au(111) clearly indicates the same redox behavior. In Figure 3a, upon potential increase to 0.51 V, a characteristic sharp peak A^I appears at 8981.4 eV. We tentatively assign this feature to the formation of Cu_2O. We note that this oxidation is limited to the near-surface region of the Cu deposit, since a shoulder corresponding to the A^0 feature from metallic Cu can still be distinguished, as well as postedge features from both expanded and relaxed Cu^0. The latter are much more pronounced than the postedge features in the HERFD XAS of pure Cu_2O[56] and therefore dominate the spectral shape at high energies.

Further potential increase causes oxidation of Cu_2O to CuO, which can be clearly identified in Figure 3a by a strong resonance at 8997 eV, a shift of the main absorption edge to higher energy, and a new postedge feature B^{II} at 9015 eV. Even at 0.71 V, however, Cu oxidation remains incomplete. Additional intensity at the B^0 energies is still apparent and diminishes a peak that is expected for CuO at 8987 eV[56] to a shoulder. On the basis of the height of the shoulder at 8980.5 eV, we estimate that ∼25% of the Cu atoms remain in the metallic or Cu(I) states.

The redox behavior of a single Cu monolayer on Au(111) is markedly different from that of thick Cu electrodes, as can be seen in its potential-dependent HERFD XAS (Figure 3b). Even though much narrower intervals between potentials were chosen here than with 7 ML Cu/Au(111), the complete absence of feature A^I indicates that no Cu(I) species is formed, but instead a direct transition from Cu(0) to Cu(II) becomes apparent with the decrease of Cu(0) features and the growth of peaks A^{II} and B^{II}. Likewise, when we measured HERFD XAS as a function of decreasing potentials, we were able to detect the presence of Cu_2O with 7 ML Cu/Au(111) (Figure 3a) but not with 1 ML Cu/Au(111) (Figure 3b). This finding also explains why only one pair of broad peaks is observed in the cyclic voltammogram of 1 ML Cu/Au(111) (Figure 4), instead of two well-separated peak pairs for the Cu(0)/Cu(I) and Cu(I)/Cu(II) transitions, as consistently observed with thick Cu electrodes[49] and also with 7 ML Cu/Au(111).

dx.doi.org/10.1021/jp412000j | J. Phys. Chem. C 2014, 118, 7954−7961

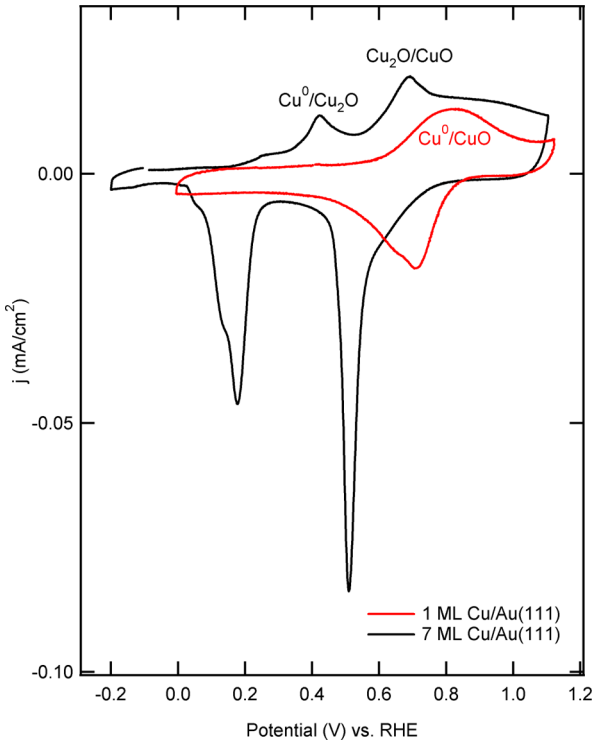

Figure 4. Comparison of cyclic voltammograms of Cu/Au(111), recorded with dE/dt = 10 mV/s. The strongly different redox behavior of 1 ML Cu (red curve) and 7 ML Cu (black curve) can be clearly seen.

We note a striking similarity between our findings for 1 ML Cu/Au(111) and a study of 1 ML Cu on Pt nanoparticles in a similar electrolyte (0.1 M NaOH).[57] The CVs of Cu/Au(111) and Cu/Pt in alkaline electrolyte have almost identical shapes and, if considered on the RHE potential scale, peak positions. This similarity suggests a common physical origin that could affect the phase transformations of a single Cu layer. First, we note that both Au and Pt surfaces undergo Cu underpotential deposition in acidic electrolytes.[58] Metal upd layers are subject to additional stabilization compared to bulk metals through a combination of interactions of the metal adatoms with the substrate and with electrolyte anions. In the case of upd Cu layers on Au and platinum group metal surfaces, a general tendency of the Cu layer toward significantly larger Cu−Cu distances than in bulk Cu can be observed,[30,59−61] since the Cu atoms form either pseudomorphic (1 × 1) overlayers or "2D compound"-like layers in which Cu atoms are in registry with a top layer of anions.[58] DFT calculations on the adsorption and dissociation of O_2 on Cu(111) predict that increased Cu−Cu distances result in a reduction of the effects of compressive strain and adsorbate−adsorbate repulsion.[62] This could increase the critical coverage above which further uptake of electrolyte species takes place through either metal−nonmetal place-exchange (compound formation) or Cu dissolution. Moreover, 0.68 eV (0.46 eV) stronger Cu−O binding energies have been calculated for Cu monolayers on Au (Pt) than on pure Cu.[63] One could therefore speculate that the stabilization of the metallic Cu monolayer on Au or Pt due to an OH coverage greater than the saturation coverage on Cu(111) could become thermodynamically more favorable than the formation of Cu_2O.

It is noteworthy that even the oxidation of 1 ML Cu/Au(111) remains incomplete up to a potential of 0.86 V. In Figure 3b, the spectrum taken at 0.86 V shows an even greater contribution from residual Cu^0 than that of the oxidized multilayer sample (Figure 3a). While in the multilayer case the presence of Cu^0 at high potentials can be simply explained with passivation, such an effect seems unlikely for a single Cu layer if each Cu atom is exposed to electrolyte. Instead, we assign the Cu^0 fraction in the oxidized monolayer sample to Cu atoms that have undergone place-exchange with substrate Au atoms. Furthermore, we observe that cathodic reduction of the CuO layer, which we followed with HERFD XAS to −0.28 V, is accompanied by an increase of a Cu^0 fraction that is inert to oxidation at high potentials: subsequent HERFD XAS measurements at 0.91 V indicate an even larger Cu^0 component than the initial measurement of the oxidized Cu layer (Figure 5).

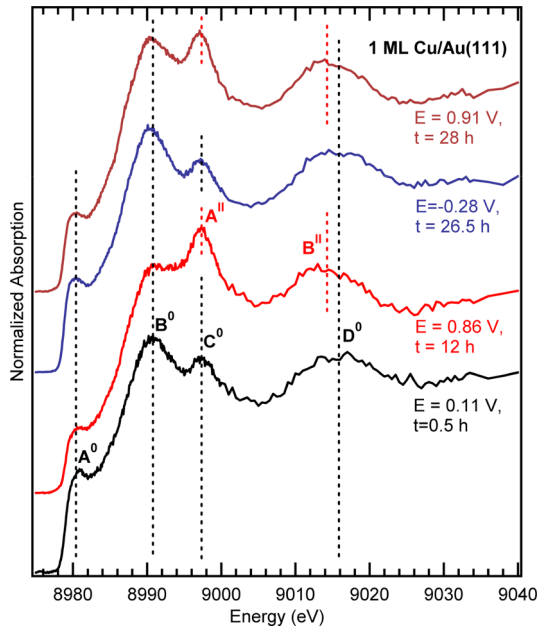

Figure 5. HERFD XAS of 1 ML Cu/Au(111) taken during two subsequent cycles of electrooxidation and electroreduction. The second measurement at high potential indicates a higher amount of residual Cu^0. The features A^0, B^0, C^0, and D^0 indicate the presence of Cu^0; features A^{II} and B^{II} are characteristic for CuO.

Although we find it necessary to further investigate the influence of electrochemical parameters in much more detail, we identify two particular conditions that could be expected to accelerate interfacial Cu/Au alloy formation:

(i) OH desorption at very low potentials would leave behind the highly strained pseudomorphic Cu monolayer without any stabilizing adsorbates. Pure Cu already has higher surface energy than Au;[44] this will be exacerbated by the 12.5% expansion of a single Cu layer. Segregation of Au resulting in an Au-rich termination would therefore minimize the surface energy.

(ii) The initial stages of CuO reduction could produce isolated "stranded" Cu atoms that lack the sufficient number of Cu^0 neighbors to grow stable Cu islands and will therefore be incorporated into the Au lattice.

To date, comparable measurements probing the behavior of ultrathin Cu layers in the submonolayer to monolayer range on Au(111) electrodes at such low potentials as studied here have

dx.doi.org/10.1021/jp412000j | J. Phys. Chem. C 2014, 118, 7954−7961

been scarce.[7,64] Most of the known studies of upd Cu layers so far have only addressed conditions where the Cu layers are subject to strong interactions with coadsorbed anions. The measurements presented here show a Cu monolayer at an Au/electrolyte interface that is not significantly influenced by anion adsorption. Therefore, the substrate-induced strain of the Cu layer becomes much more important. In order to minimize strain, place-exchange between Cu and Au atoms occurs. A well-conceivable alternative mechanism, formation of a more close-packed incommensurate Cu layer, is not supported by our HERFD XAS data.

Since it is well-known that oxygen adsorption[23] and anodic dissolution of Cu,[18,20,21] which can be assumed to involve an intermediate interaction of Cu atoms with oxygen-containing adsorbates or with halides,[19,22] is a strong driving force for surface segregation of Cu atoms from Cu/Au alloys, one could expect that exposure of 1 ML Cu/Au(111) to anodic potentials in 0.01 M NaOH would also result in a reversal of subsurface alloy formation. The incomplete oxidation of the Cu monolayer even at significant overpotential indicates that the tendency for subsurface Cu to respond to oxidizing conditions is rather low. We conjecture that the overall lower concentration of subsurface Cu resulting from a starting configuration of 1 ML Cu on a pure Au substrate instead of a bulk Cu/Au alloy with much higher subsurface Cu concentration makes dealloying entropically less favorable. Furthermore, oxidation results in the formation of a CuO overlayer instead of anodic dissolution. While dissolution sustains the driving force for Cu segregation by continuous removal of Cu surface atoms, the CuO overlayer formed in alkaline electrolyte may have a passivating effect.

CONCLUSIONS

In situ HERFD XAS shows a strong difference of the potential-dependent behavior of a single Cu layer from bulk Cu electrodes. For 1 ML Cu/Au(111), and also 1 ML Cu/Pt,[57] only one redox transition between a hydroxide-modified Cu layer and a Cu(II) oxide is observed, instead of, as commonly observed with thick Cu electrodes, two separate transitions between a hydroxide-modified Cu surface, Cu(I) oxide, and Cu(II) oxide. The overall onset of Cu oxidation is also significantly shifted anodically.

The significant tensile strain of a single Cu monolayer on Au, Pt, and platinum-group metals in general could be expected to drastically alter not only the redox behavior of Cu as observed here but also the interaction of Cu with CO_2 reduction intermediates. Promising indications have been reported that tensile strain could indeed be utilized to control the selectivity for methane vs ethylene formation.[5] However, the stability of strained bimetallic catalysts under operating conditions needs to be investigated carefully. In the present case, alloying of Cu with the Au(111) substrate is observed to occur for both monolayer and multilayer Cu deposits. We therefore expect that any possible effect of "tuning" the interactions between a strained Cu surface layer and CO_2 reduction intermediates would occur only temporarily and would later be superseded by the characteristics of an Au-rich alloy.

AUTHOR INFORMATION

Corresponding Author

*E-mail dfriebel@slac.stanford.edu (D.F.).

Notes

The authors declare no competing financial interest.

ACKNOWLEDGMENTS

This material is based upon work supported by the Air Force Office of Scientific Research through the MURI program under AFOSR Award FA9550-10-1-0572. This research was partly carried out at the Stanford Synchrotron Radiation Lightsource, a National User Facility operated by Stanford University on behalf of the U.S. Department of Energy, Office of Basic Energy Sciences. We thank Uwe Bergmann for valuable discussions of the HERFD XAS technique.

REFERENCES

(1) Hori, Y. Electrochemical CO_2 Reduction on Metal Electrodes. In *Modern Aspects of Electrochemistry*; Vayenas, C. G., White, R. E., Gamboa-Aldeco, M. E., Eds.; Modern Aspects of Electrochemistry; Springer: New York, 2008; pp 89−189.

(2) Kuhl, K. P.; Cave, E. R.; Abram, D. N.; Jaramillo, T. F. New Insights into the Electrochemical Reduction of Carbon Dioxide on Metallic Copper Surfaces. *Energy Environ. Sci.* **2012**, *5*, 7050−7059.

(3) Tang, W.; Peterson, A. A.; Varela, A. S.; Jovanov, Z. P.; Bech, L.; Durand, W. J.; Dahl, S.; Nørskov, J. K.; Chorkendorff, I. The Importance of Surface Morphology in Controlling the Selectivity of Polycrystalline Copper for CO_2 Electroreduction. *Phys. Chem. Chem. Phys.* **2012**, *14*, 76.

(4) Li, C. W.; Kanan, M. W. CO_2 Reduction at Low Overpotential on Cu Electrodes Resulting from the Reduction of Thick Cu_2O Films. *J. Am. Chem. Soc.* **2012**, *134*, 7231−7234.

(5) Reske, R.; Duca, M.; Oezaslan, M.; Schouten, K. J. P.; Koper, M. T. M.; Strasser, P. Controlling Catalytic Selectivities during CO_2 Electroreduction on Thin Cu Metal Overlayers. *J. Phys. Chem. Lett.* **2013**, *4*, 2410−2413.

(6) Christophe, J.; Doneux, T.; Buess-Herman, C. Electroreduction of Carbon Dioxide on Copper-Based Electrodes: Activity of Copper Single Crystals and Copper−Gold Alloys. *Electrocatalysis* **2012**, *3*, 139−146.

(7) Schlaup, C.; Horch, S. In-Situ STM Study of Phosphate Adsorption on Cu(111), Au(111) and Cu/Au(111) Electrodes. *Surf. Sci.* **2013**, *608*, 44−54.

(8) Friebel, D.; Viswanathan, V.; Miller, D. J.; Anniyev, T.; Ogasawara, H.; Larsen, A. H.; O'Grady, C. P.; Nørskov, J. K.; Nilsson, A. Balance of Nanostructure and Bimetallic Interactions in Pt Model Fuel Cell Catalysts: In Situ XAS and DFT Study. *J. Am. Chem. Soc.* **2012**, *134*, 9664−9671.

(9) Maroun, F.; Ozanam, F.; Magnussen, O. M.; Behm, R. J. The Role of Atomic Ensembles in the Reactivity of Bimetallic Electrocatalysts. *Science* **2001**, *293*, 1811−1814.

(10) Jirkovský, J. S.; Panas, I.; Ahlberg, E.; Halasa, M.; Romani, S.; Schiffrin, D. J. Single Atom Hot-Spots at Au−Pd Nanoalloys for Electrocatalytic H_2O_2 Production. *J. Am. Chem. Soc.* **2011**, *133*, 19432−19441.

(11) Jirkovský, J. S.; Panas, I.; Romani, S.; Ahlberg, E.; Schiffrin, D. J. Potential-Dependent Structural Memory Effects in Au−Pd Nanoalloys. *J. Phys. Chem. Lett.* **2012**, *3*, 315−321.

(12) Peterson, A. A.; Nørskov, J. K. Activity Descriptors for CO_2 Electroreduction to Methane on Transition-Metal Catalysts. *J. Phys. Chem. Lett.* **2012**, *3*, 251−258.

(13) Russell, A. E.; Rose, A. X-Ray Absorption Spectroscopy of Low Temperature Fuel Cell Catalysts. *Chem. Rev.* **2004**, *104*, 4613−4636.

(14) Friebel, D.; Miller, D. J.; Nordlund, D.; Ogasawara, H.; Nilsson, A. Degradation of Bimetallic Model Electrocatalysts: An In Situ X-Ray Absorption Spectroscopy Study. *Angew. Chem., Int. Ed.* **2011**, *50*, 10190−10192.

(15) Friebel, D.; Miller, D. J.; O'Grady, C. P.; Anniyev, T.; Bargar, J.; Bergmann, U.; Ogasawara, H.; Wikfeldt, K. T.; Pettersson, L. G. M.; Nilsson, A. In Situ X-Ray Probing Reveals Fingerprints of Surface Platinum Oxide. *Phys. Chem. Chem. Phys.* **2011**, *13*, 262−266.

(16) Merte, L. R.; Behafarid, F.; Miller, D. J.; Friebel, D.; Cho, S.; Mbuga, F.; Sokaras, D.; Alonso-Mori, R.; Weng, T.-C.; Nordlund, D.;

et al. Electrochemical Oxidation of Size-Selected Pt Nanoparticles Studied Using in Situ High-Energy-Resolution X-Ray Absorption Spectroscopy. *ACS Catal.* **2012**, *2*, 2371−2376.
(17) Friebel, D.; Bajdich, M.; Yeo, B. S.; Louie, M.; Miller, D. J.; Casalongue, H. S.; Mbuga, F.; Weng, T.-C.; Nordlund, D.; Sokaras, D.; et al. On the Chemical State of Co Oxide Electrocatalysts during Alkaline Water Splitting. *Phys. Chem. Chem. Phys.* **2013**, in press.
(18) Renner, F. U.; Stierle, A.; Dosch, H.; Kolb, D. M.; Lee, T.-L.; Zegenhagen, J. Initial Corrosion Observed on the Atomic Scale. *Nature* **2006**, *439*, 707−710.
(19) Renner, F. U.; Stierle, A.; Dosch, H.; Kolb, D. M.; Zegenhagen, J. The Influence of Chloride on the Initial Anodic Dissolution of $Cu_3Au(111)$. *Electrochem. Commun.* **2007**, *9*, 1639−1642.
(20) Renner, F. U.; Stierle, A.; Dosch, H.; Kolb, D. M.; Lee, T. L.; Zegenhagen, J. In Situ X-Ray Diffraction Study of the Initial Dealloying and Passivation of $Cu_3Au(111)$ during Anodic Dissolution. *Phys. Rev. B* **2008**, *77*, 235433.
(21) Pareek, A.; Borodin, S.; Bashir, A.; Ankah, G. N.; Keil, P.; Eckstein, G. A.; Rohwerder, M.; Stratmann, M.; Gründer, Y.; Renner, F. U. Initiation and Inhibition of Dealloying of Single Crystalline Cu_3Au (111) Surfaces. *J. Am. Chem. Soc.* **2011**, *133*, 18264−18271.
(22) Ankah, G. N.; Pareek, A.; Cherevko, S.; Topalov, A. A.; Rohwerder, M.; Renner, F. U. The Influence of Halides on the Initial Selective Dissolution of Cu_3Au (111). *Electrochim. Acta* **2012**, *85*, 384−392.
(23) Völker, E.; Williams, F. J.; Calvo, E. J.; Jacob, T.; Schiffrin, D. J. O_2 Induced Cu Surface Segregation in Au−Cu Alloys Studied by Angle Resolved XPS and DFT Modelling. *Phys. Chem. Chem. Phys.* **2012**, *14*, 7448.
(24) Andersson, K. J.; Calle-Vallejo, F.; Rossmeisl, J.; Chorkendorff, I. Adsorption-Driven Surface Segregation of the Less Reactive Alloy Component. *J. Am. Chem. Soc.* **2011**, *131*, 2404−2407.
(25) Sokaras, D.; Weng, T.-C.; Nordlund, D.; Alonso-Mori, R.; Velikov, P.; Wenger, D.; Garachtchenko, A.; George, M.; Borzenets, V.; Johnson, B.; et al. A Seven-Crystal Johann-Type Hard X-Ray Spectrometer at the Stanford Synchrotron Radiation Lightsource. *Rev. Sci. Instrum.* **2013**, *84*, 053102−053102−8.
(26) Glatzel, P.; Bergmann, U. High Resolution 1s Core Hole X-Ray Spectroscopy in 3d Transition Metal Complexes - Electronic and Structural Information. *Coord. Chem. Rev.* **2005**, *249*, 65−95.
(27) Waychunas, G. A. Grazing-Incidence X-Ray Absorption and Emission Spectroscopy. In *Reviews in Mineralogy and Geochemistry*; Mineralogical Society of America: Chantilly, VA, 2002; Vol. *49*, pp 267−315.
(28) Gründer, Y.; Thompson, P.; Brownrigg, A.; Darlington, M.; Lucas, C. A. Probing the Halide−Metal Interaction by Monolayer Metal Deposition at the Electrochemical Interface. *J. Phys. Chem. C* **2012**, *116*, 6283−6288.
(29) Nakamura, M.; Endo, O.; Ohta, T.; Ito, M.; Yoda, Y. Surface X-Ray Diffraction Study of Cu UPD on Au(111) Electrode in 0.5 M H_2SO_4 Solution: The Coadsorption Structure of UPD Copper, Hydration Water Molecule and Bisulfate Anion on Au(111). *Surf. Sci.* **2002**, *514*, 227−233.
(30) Toney, M. F.; Howard, J. N.; Richer, J.; Borges, G. L.; Gordon, J. G.; Melroy, O. R.; Yee, D.; Sorensen, L. B. Electrochemical Deposition of Copper on a Gold Electrode in Sulfuric Acid: Resolution of the Interfacial Structure. *Phys. Rev. Lett.* **1995**, *75*, 4472−4475.
(31) Shi, Z.; Wu, S.; Lipkowski, J. Coadsorption of Metal Atoms and Anions: Cu UPD in the Presence of SO_4^{2-}, Cl^- and Br^-. *Electrochim. Acta* **1995**, *40*, 9−15.
(32) Hotlos, J.; Magnussen, O. M.; Behm, R. J. Effect of Trace Amounts of Cl^- in Cu Underpotential Deposition on Au(111) in Perchlorate Solutions: An in-Situ Scanning Tunneling Microscopy Study. *Surf. Sci.* **1995**, *335*, 129−144.
(33) Friebel, D.; Schlaup, C.; Broekmann, P.; Wandelt, K. Sulfidation of a Cu Submonolayer at the Au(111)/Electrolyte Interface - An in Situ STM Study. *Surf. Sci.* **2006**, *600*, 2800−2809.
(34) Friebel, D.; Schlaup, C.; Broekmann, P.; Wandelt, K. Copper Sulfide Nanostripe Patterns at the Au(111)/Electrolyte Interface Studied by in Situ STM. *Phys. Chem. Chem. Phys.* **2007**, *9*, 2142−2145.
(35) Schlaup, C.; Spaenig, A.; Broekmann, P.; Wandelt, K. Sulfide Anion Interaction with Cu(100) and Cu Modified Au(100): An Electrochemical STM Study. *Phys. Status Solidi A* **2010**, *207*, 254−260.
(36) Eisenberger, P.; Platzman, P. M.; Winick, H. X-Ray Resonant Raman Scattering: Observation of Characteristic Radiation Narrower Than the Lifetime Width. *Phys. Rev. Lett.* **1976**, *36*, 623−626.
(37) Hämäläinen, K.; Siddons, D. P.; Hastings, J. B.; Berman, L. E. Elimination of the Inner-Shell Lifetime Broadening in X-Ray-Absorption Spectroscopy. *Phys. Rev. Lett.* **1991**, *67*, 2850−2853.
(38) Safonova, O. V.; Tromp, M.; van Bokhoven, J. A.; de Groot, F. M. F.; Evans, J.; Glatzel, P. Identification of CO Adsorption Sites in Supported Pt Catalysts Using High-Energy-Resolution Fluorescence Detection X-Ray Spectroscopy. *J. Phys. Chem. B* **2006**, *110*, 16162−16164.
(39) Bianconi, A.; Fritsch, E.; Calas, G.; Petiau, J. X-Ray-Absorption Near-Edge Structure of 3d Transition Elements in Tetrahedral Coordination: The Effect of Bond-Length Variation. *Phys. Rev. B* **1985**, *32*, 4292−4295.
(40) Sette, F.; Stöhr, J.; Hitchcock, A. P. Correlation between Intramolecular Bond Lengths and K-Shell Σ-Shape Resonances in Gas-Phase Molecules. *Chem. Phys. Lett.* **1984**, *110*, 517−520.
(41) Stöhr, J.; Sette, F.; Johnson, A. L. Near-Edge X-Ray-Absorption Fine-Structure Studies of Chemisorbed Hydrocarbons: Bond Lengths with a Ruler. *Phys. Rev. Lett.* **1984**, *53*, 1684−1687.
(42) Bearden, J. A.; Burr, A. F. Reevaluation of X-Ray Atomic Energy Levels. *Rev. Mod. Phys.* **1967**, *39*, 125−142.
(43) Nichols, R. J.; Bunge, E.; Meyer, H.; Baumgärtel, H. Classification of Growth Behaviour for Copper on Various Substrates with in-Situ Scanning Probe Microscopy. *Surf. Sci.* **1995**, *335*, 110−119.
(44) Bauer, E.; van der Merwe, J. H. Structure and Growth of Crystalline Superlattices - From Monolayer to Superlattice. *Phys. Rev. B* **1986**, *33*, 3657−3671.
(45) Strehblow, H.-H.; Titze, B. The Investigation of the Passive Behaviour of Copper in Weakly Acid and Alkaline Solutions and the Examination of the Passive Film by ESCA and ISS. *Electrochim. Acta* **1980**, *25*, 839−850.
(46) Kautek, W.; Gordon, J. G. XPS Studies of Anodic Surface Films on Copper Electrodes. *J. Electrochem. Soc.* **1990**, *137*, 2672−2677.
(47) Millet, B.; Fiaud, C.; Hinnen, C.; Sutter, E. M. M. A Correlation between Electrochemical Behaviour, Composition and Semiconducting Properties of Naturally Grown Oxide Films on Copper. *Corros. Sci.* **1995**, *37*, 1903−1918.
(48) Maurice, V.; Strehblow, H.-H.; Marcus, P. In Situ STM Study of the Initial Stages of Oxidation of Cu(111) in Aqueous Solution. *Surf. Sci.* **2000**, *458*, 185−194.
(49) Kunze, J.; Maurice, V.; Klein, L. H.; Strehblow, H.-H.; Marcus, P. In Situ STM Study of the Duplex Passive Films Formed on Cu(111) and Cu(001) in 0.1 M NaOH. *Corros. Sci.* **2004**, *46*, 245−264.
(50) Friebel, D.; Broekmann, P.; Wandelt, K. Electrochemical in Situ STM Study of a Cu(111) Electrode in Neutral Sulfate Containing Electrolyte. *Phys. Status Solidi A* **2004**, *201*, 861−869.
(51) Chu, Y. S.; Robinson, I. K.; Gewirth, A. A. Comparison of Aqueous and Native Oxide Formation on Cu(111). *J. Chem. Phys.* **1999**, *110*, 5952−5959.
(52) Chan, H. Y. H.; Takoudis, C. G.; Weaver, M. J. Oxide Film Formation and Oxygen Adsorption on Copper in Aqueous Media As Probed by Surface-Enhanced Raman Spectroscopy. *J. Phys. Chem. B* **1999**, *103*, 357−365.
(53) Soon, A.; Todorova, M.; Delley, B.; Stampfl, C. Oxygen Adsorption and Stability of Surface Oxides on Cu(111): A First-Principles Investigation. *Phys. Rev. B* **2006**, *73*, 165424.
(54) Soon, A.; Todorova, M.; Delley, B.; Stampfl, C. Surface Oxides of the Oxygen−Copper System: Precursors to the Bulk Oxide Phase? *Surf. Sci.* **2007**, *601*, 5809−5813.

(55) Pourbaix, M. *Atlas of Electrochemical Equilibria in Aqueous Solutions*, 2nd ed.; NACE: Houston, 1974.
(56) Kleymenov, E.; Sa, J.; Abu-Dahrieh, J.; Rooney, D.; Bokhoven, J. A. van; Troussard, E.; Szlachetko, J.; Safonova, O. V.; Nachtegaal, M. Structure of the Methanol Synthesis Catalyst Determined by in Situ HERFD XAS and EXAFS. *Catal. Sci. Technol.* **2012**, *2*, 373−378.
(57) Borthen, P.; Hwang, B.-J.; Strehblow, H.-H.; Kolb, D. M. In Situ Observation of the Potential-Dependent Chemical State and Structure of a Cu Monolayer Deposited on the Surface of Carbon-Supported Platinum Clusters. *J. Phys. Chem. B* **2000**, *104*, 5078−5083.
(58) Herrero, E.; Buller, L. J.; Abruña, H. D. Underpotential Deposition at Single Crystal Surfaces of Au, Pt, Ag and Other Materials. *Chem. Rev.* **2001**, *101*, 1897−1930.
(59) Melroy, O. R.; Samant, M. G.; Borges, G. L.; Gordon, J. G.; Blum, L.; White, J. H.; Albarelli, M. J.; McMillan, M.; Abruna, H. D. In-Plane Structure of Underpotentially Deposited Copper on Gold(111) Determined by Surface EXAFS. *Langmuir* **1988**, *4*, 728−732.
(60) Yee, H. S.; Abruna, H. D. In-Situ X-Ray Studies of the Underpotential Deposition of Copper on Platinum(111). *J. Phys. Chem.* **1993**, *97*, 6278−6288.
(61) Yee, H. S.; Abruna, H. D. Ab-Initio XAFS Calculations and In-Situ XAFS Measurements of Copper Underpotential Deposition On Pt(111) - A Comparative-Study. *J. Phys. Chem.* **1994**, *98*, 6552−6558.
(62) Xu, Y.; Mavrikakis, M. Adsorption and Dissociation of O_2 on Cu(111): Thermochemistry, Reaction Barrier and the Effect of Strain. *Surf. Sci.* **2001**, *494*, 131−144.
(63) Greeley, J.; Nørskov, J. K. A General Scheme for the Estimation of Oxygen Binding Energies on Binary Transition Metal Surface Alloys. *Surf. Sci.* **2005**, *592*, 104−111.
(64) Täubert, C. E.; Petri, M.; Kolb, D. M. On a New Phase Transition in the Cu/Au(111)/H_2SO_4 System. *Z. Phys. Chem.* **2007**, *221*, 1493−1498.